Minireview

New insights into the structure and oligomeric state of the bacterial multidrug transporter EmrE: an unusual asymmetric homo-dimer

I. Ubarretxena-Belandia, C.G. Tate*

MRC Laboratory of Molecular Biology, Hills Road, Cambridge CB2 2QH, UK

Abstract **EmrE is a small multidrug transporter that contains 110 amino acid residues that form four transmembrane α-helices. The three-dimensional structure of EmrE has been determined from two-dimensional crystals by electron cryo-microscopy. EmrE is an asymmetric homo-dimer with one substrate molecule bound in a chamber accessible laterally from one leaflet of the lipid bilayer. Evidence from substrate binding analyses and analytical ultracentrifugation of detergent-solubilised EmrE shows that the minimum functional unit for substrate binding is a dimer. However, it is possible that EmrE exists as a tetramer in vivo and plausible models are suggested based upon analyses of two-dimensional crystals.**
© 2004 Federation of European Biochemical Societies. Published by Elsevier B.V. All rights reserved.

Key words: Asymmetry; Electron crystallography; Membrane protein; Multidrug; Structure

1. Introduction

The incidence of Gram-negative pathogens resistant to a large range of antibiotics is increasing and the resultant deficit in effective therapeutic strategies emphasises the urgent need for novel therapeutic approaches to the treatment of infectious disease [1]. To a large extent, multidrug and drug-specific efflux systems in these pathogenic bacteria account for their clinically significant resistance to therapeutic compounds, and consequently have attracted the attention of many research groups [2,3]. The efflux of toxic molecules is driven either by ATP hydrolysis, as in the ABC transporter superfamily, or by coupling efflux to the inward movement of protons down their concentration gradient in an antiport mechanism. H^+-drug antiporters have evolved in many different transporter families [4], including the major facilitator superfamily, the resistance–nodulation–cell division family and the small multidrug resistance (SMR) family. The SMR family is composed of polytopic integral membrane proteins about 100–110 amino acids long that form four putative transmembrane α-helices [4]. So far more than 60 genes encoding SMR proteins have been identified in bacteria and archaebacteria, many of which are pathogenic organisms [5]. EmrE, a SMR representative of *Escherichia coli*, has been extensively studied and serves as the archetype for the whole family [6]. EmrE catalyses the electrogenic efflux of a wide variety of cationic aromatic hydrocarbons of varying size, structure and charge, thereby rendering *E. coli* resistant to these compounds [7]. Recent structural studies by electron cryo-microscopy (cryo-EM) of two-dimensional (2D) crystals of purified EmrE reconstituted in proteoliposomes have revealed the three-dimensional (3D) architecture of the protein, including the location of the substrate binding site, and the translocation pathway within the protein [8–10]. The most remarkable feature of the structure of EmrE is that it is a homo-dimer composed of eight transmembrane α-helices arranged asymmetrically, a feature never observed before for membrane proteins. In this review the current knowledge on EmrE will be summarised and discussed with emphasis on its structure and oligomeric state.

2. Biochemical properties

Assays in whole cells have shown that EmrE behaves as a multidrug transporter and catalyses the efflux of a wide variety of cationic aromatic hydrocarbons of varying size, structure and charge, such as methyl viologen, ethidium acriflavine, tetracycline and tetraphenylphosphonium (TPP^+) [7,11,12]. EmrE has been purified using either organic solvents [7] or detergents [13] and reconstituted into phospholipid bilayers and these proteoliposomes are capable of accumulating [^{14}C]methyl viologen by using a proton electrochemical gradient. One useful property of EmrE is that it can be extracted from membranes in a virtually pure form using chloroform–methanol solutions, which allowed the development of a rapid and simple reconstitution assay that has been used in many of the experiments discussed below [7].

Cysteine scanning mutagenesis experiments indicate that EmrE is composed of a tightly packed bundle of α-helices without any continuous aqueous domains, suggesting that substrates are translocated through a hydrophobic pathway in the protein [14]. Further insights into the identity of the amino acid residues in the substrate binding pocket and translocation pathway have been provided by site-directed mutagenesis and chemical modification experiments. Seven of the eight charged amino acid residues in EmrE are located in putative loops and can be replaced with either cysteine or other amino acids bearing the same charge without significantly affecting transport activity [15]. The other charged residue is Glu14, which is absolutely conserved in all EmrE ho-

*Corresponding author. Fax: (44)-1223-213556.
E-mail address: cgt@mrc-lmb.cam.ac.uk (C.G. Tate).

mologues and is located approximately in the centre of the first putative transmembrane domain (TMD 1) [5]; this residue is essential for activity and constitutes the site at which both protons and cationic substrates bind in a mutually exclusive fashion [15–17]. In addition, residues that are predicted to be on the same face of TMD 1 as Glu14 are also essential for efficient H$^+$-driven methyl viologen uptake into proteoliposomes and cells [18]. In the proposed mechanism of transport, Glu14 residues from both monomers bind the substrate, resulting in a conformation change so that the binding pocket faces the periplasm; proton binding to both Glu14 residues then induces the release of the substrate [15]. Recent data from spin labelling studies confirm that TMDs 1 from each monomer are in close proximity to each other [19]. Systematic mutation of amino acid residues in TMD 2 and TMD 3 suggests that these regions of EmrE are involved in substrate recognition, but they are not absolutely essential for drug transport [14]. No mutations to any residue in TMD 4 affected substrate recognition or transport [20]. Amino acid residues that cause decreased expression of EmrE have been found in TMDs 2, 3 and 4, but not in TMD 1 [14,20].

3. Structural analysis

Since EmrE is a well-studied representative of the SMR family and is small and apparently simple, the structure of EmrE has received considerable attention over the last decade. Hydropathy analysis of EmrE predicted four transmembrane α-helices [7]. Given the relatively short length of EmrE (110 amino acids), this suggested that about 80% of the amino acids are in helical conformation, a value that was supported by evidence from Fourier transform infrared experiments of EmrE reconstituted in lipid bilayers [21]. Further support was provided by heteronuclear nuclear magnetic resonance spectroscopy studies on the whole protein in chloroform/methanol/water mixtures [22] although EmrE is monomeric in this solvent [23]. Because of the absence of any distinctive distribution of positive charges in EmrE to suggest an orientation more likely to face the cytoplasm according to the 'positive inside' rule [24], the topology of EmrE in the membrane is unclear and has yet to be determined unambiguously.

So far, the most detailed structural information on EmrE has been provided by cryo-EM of 2D crystals. A projection structure of EmrE at 7.0 Å resolution was determined from 2D crystals obtained after reconstitution of purified His-tagged EmrE at low lipid/protein ratios in dimyristoylphosphatidylcholine bilayers [8]. The repetitive unit in the crystal was composed of eight α-helices arranged in an asymmetric manner, indicating that the minimal functional unit for EmrE was a dimer (Fig. 1B). EmrE in these 2D crystals is fully functional as shown by the high-affinity binding of [^{3}H]TPP$^+$ when saturation binding experiments were performed on them (Fig. 1A). We can conclude that TPP$^+$ binds to the EmrE within the crystals, and not just to a small non-crystalline sub-population, because all the 2D crystals became disordered after the addition of TPP$^+$ [9]. Only one crystal from the TPP$^+$ soak was sufficiently ordered to allow indexing of the diffraction pattern, and this showed that the planar space group had changed from c222 to p2, indicating that a change in EmrE conformation had occurred. Well-ordered 2D crystals of TPP$^+$-bound EmrE were grown by dialysis of detergent-solubilised EmrE in the presence of excess TPP$^+$, and
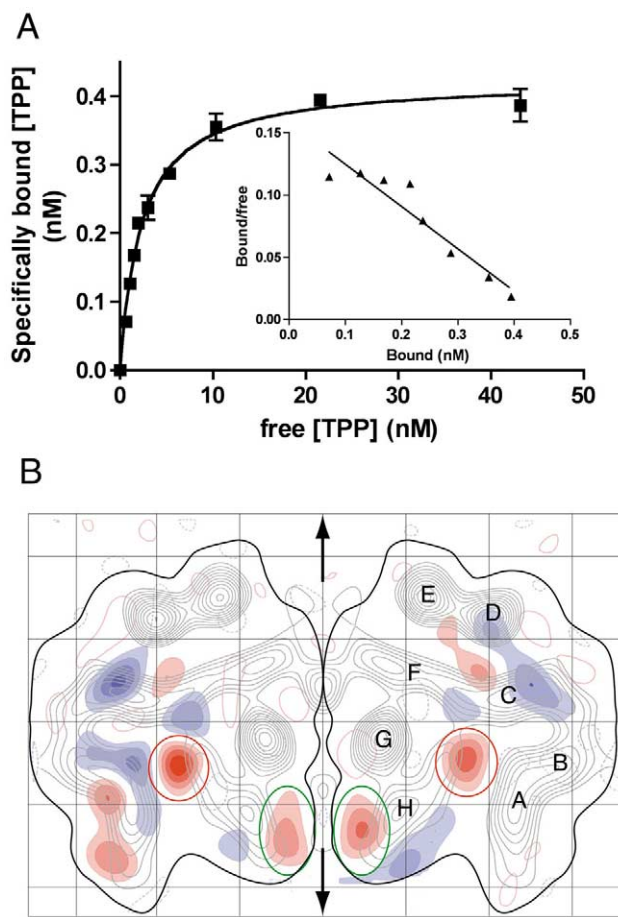

Fig. 1. A: Saturation binding curve and Scatchard analysis (inset) of [^{3}H]TPP$^+$ binding to 2D crystals (c222) of EmrE. A representative experiment is shown performed in duplicate ($K_d = 2.3 \pm 0.2$ nM). B: Density differences between native EmrE and TPP$^+$-bound EmrE. The crystallographic tetramer (grey contours) from the c222 projection map is shown overlaid with positive density differences (red contours) and negative differences (blue contours) calculated from a subtraction of the projection map for native EmrE from a projection map of TPP$^+$-bound EmrE. The two asymmetric dimers are outlined and the density difference representing TPP$^+$ is ringed by a red circle and the density difference arising from a conformation change caused by TPP$^+$ binding is ringed by a green circle. Features in the projection map are labelled according to the helix nomenclature in Fig. 2. Adapted from [9] with permission.

these crystals were also found to have p2 symmetry [9]. Two separate p2 projection maps of TPP$^+$-bound EmrE were determined from two independent crystallisation experiments and averaged; an averaged native EmrE projection structure calculated from the c222 and p222$_1$ crystals was then carefully subtracted from the averaged TPP$^+$-bound form to create a difference density map. The interpretation of this difference density image suggested that TPP$^+$ bound at the centre of the EmrE dimer, and resulted in a small movement of at least one tilted transmembrane α-helix (Fig. 1B).

Recently, the three-dimensional structure of EmrE was determined to an in-plane resolution of 7.5 Å by cryo-EM using the p2 crystals of TPP$^+$-bound EmrE [10]. The structure corresponded to an EmrE dimer composed of eight transmembrane α-helices (Fig. 2) which, when viewed along an axis perpendicular to the membrane, looked identical to the previously determined projection maps. Six tilted α-helices
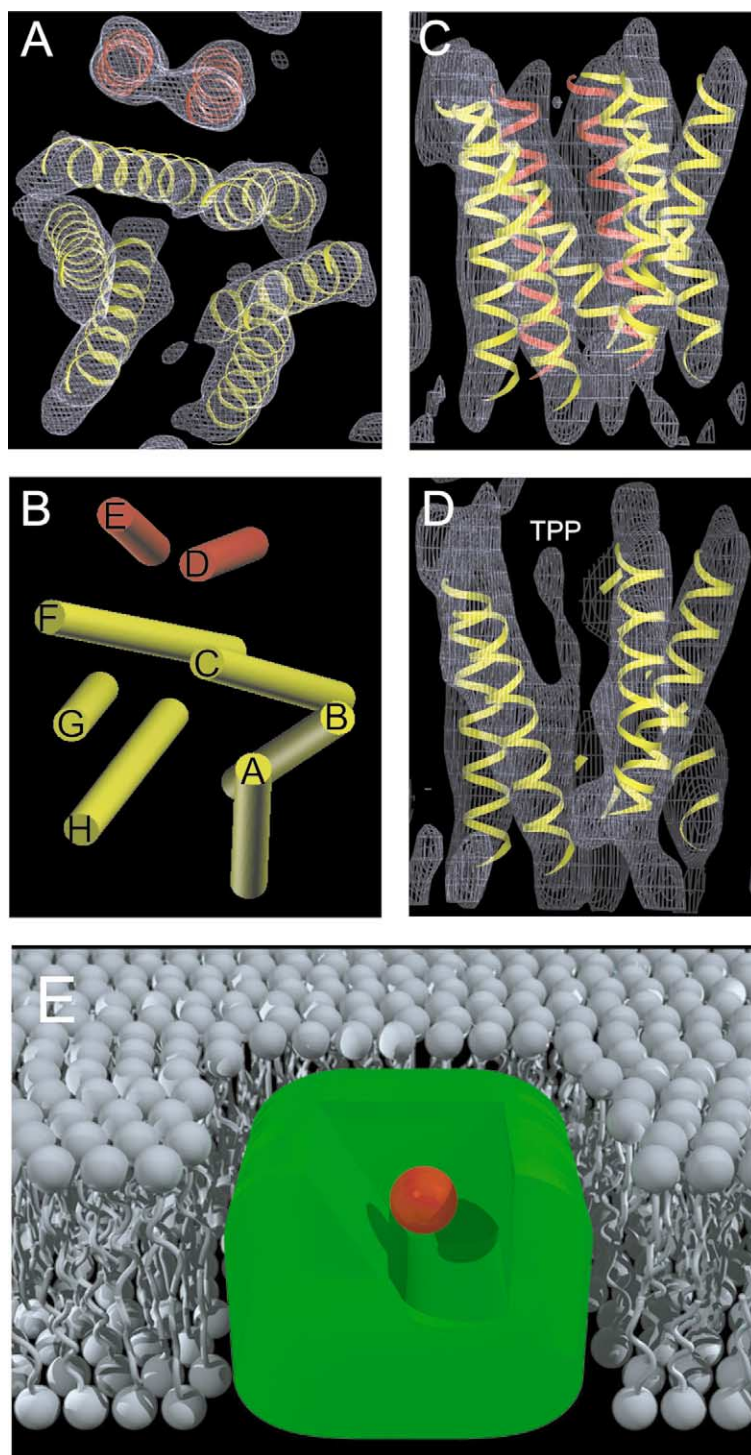
Fig. 2. 3D structure of EmrE. A: View perpendicular to the membrane plane. B: Schematic view of EmrE perpendicular to the membrane plane with α-helices represented as cylinders. C: View along the membrane plane. D: Slice through the structure viewed along the membrane plane to emphasise the density representing TPP$^+$. Idealised helices (ribbons) were manually inserted into the density (mesh) without refinement. Yellow helices form the substrate binding chamber whereas the two red helices are not in contact with TPP$^+$. E: Schematic model of EmrE showing the access to the substrate binding chamber laterally from one leaflet of the lipid bilayer and from the aqueous medium. TPP$^+$ is represented as a red sphere. Reproduced from [10] with permission from Oxford University Press.

formed the walls of a chamber in which TPP$^+$ was bound. The remaining two α-helices were nearly perpendicular to the membrane and were separated from the TPP$^+$ binding chamber by two of the highly tilted helices in the wall. The chamber extends from one surface of the membrane to just past the

membrane centre, where it appears to be closed by the convergence of helices F and H. The density for TPP$^+$ appears as an elongated mass, merging to the main density for helix H, rather than as the predicted sphere, because the effective resolution of the structure perpendicular to the membrane plane

is only 16 Å. The substrate binding chamber has two openings, one facing the aqueous medium and the other facing laterally the lipid bilayer (Fig. 2E), which would allow hydrophobic substrates in one leaflet of the *E. coli* inner membrane to diffuse into the EmrE binding site. In addition, it is possible that access to the lipid bilayer between the α-helices is required for larger substrates too big to fit into the binding region defined by TPP$^+$ in the structure, thus allowing EmrE to transport a larger range of substrates.

At the current resolution of our 3D structure we cannot directly assign amino acid sequences to the observed densities. Although we have made a tentative assignment of which four densities represent each monomer, this was based upon a series of logical arguments and rationalisations [10]. We have similarly used the limited biochemical [19] and cross-linking [20] data to investigate possible models for the EmrE structure (unpublished data). Although this was instructive, we could not define one model as more likely than a small number of other possible models for two reasons. Firstly, as mentioned before, there are not enough published data to discriminate between the models. Secondly, EmrE represents a new structural paradigm for a membrane protein, so we have no prior knowledge of how two monomers of identical amino acid sequence can form an asymmetric dimer. It is probable that the structures of the EmrE monomers within the asymmetric dimer do not represent the structure of a free EmrE monomer as would occur immediately after being synthesised in the cell. Thus the monomers may only attain their final structure after dimerisation has occurred.

4. Oligomeric state

It is critically important to define the oligomeric state of a membrane protein if we are to understand how it functions, but it can be extremely difficult to determine [25]. We will consider two stages of oligomerisation based upon the interpretation of structural data from the 2D crystals. The primary oligomeric state will be defined as the number of monomers required to form a substrate binding site and translocation pathway through the membrane, but this would not necessarily be the functional unit in vivo. The secondary oligomeric state will be defined as the oligomeric order found in vivo, which could involve further oligomerisation either for reasons of stability, or because it may be an obligatory requirement for function. The importance of these distinctions in the oligomeric state is supported by good evidence to suggest that many transporters, whose primary oligomeric state is a monomer, appear to function as active transporters only once they have formed dimers or tetramers in the membrane [26–29].

Three lines of evidence show that the primary oligomeric state of EmrE is a dimer. The smallest repetitive structural unit in 2D crystals of native EmrE is an asymmetric dimer [8]. Comparison of these structural units between 2D crystals with and without TPP$^+$ bound is consistent with one TPP$^+$ molecule binding in the middle of the asymmetric dimer [9]. This is further corroborated by the 3D structure of TPP$^+$-bound EmrE [10]. In addition, TPP$^+$ binds to detergent-solubilised EmrE with high affinity in a molar ratio of 1:2 (TPP$^+$:EmrE) [9] and this preparation has been shown by analytical ultracentrifugation to be a dimer (Butler and Tate, manuscript in preparation). Both lines of biophysical evidence are supported further by biochemical data in the form of cross-linking [20]
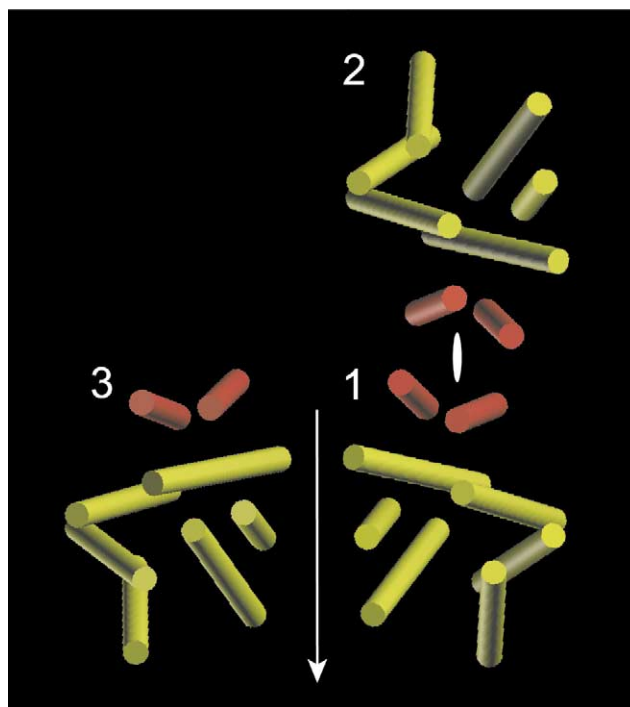

Fig. 3. EmrE forms two crystallographic tetramers in the 2D crystals, with the asymmetric dimers related either by an in-plane two-fold axis (arrow between dimers 1 and 3) or by a two-fold axis perpendicular to the membrane plane (ellipse between dimers 1 and 2). Reproduced from [10] with permission from Oxford University Press.

and hetero-oligomer formation [30] that indicate the presence of EmrE dimers in the detergent-solubilised state.

The secondary oligomeric state of EmrE in vivo is less certain. Negative-dominance studies, based upon measuring proton-driven methyl viologen uptake into proteoliposomes, clearly suggest that EmrE is present in the membrane in a higher oligomeric state than a dimer [31]. Given that the primary oligomeric state of EmrE is a dimer, then the most plausible state in vivo is therefore a tetramer, although even higher oligomeric states cannot be entirely discounted. Two tantalising possibilities for plausible EmrE tetramers are suggested from 2D projection maps, because in all three different crystal forms these tetramers are virtually identical [9]. In projection, one crystallographic tetramer (dimer 1 and 3) is related by a two-fold axis in the plane of the membrane, with the two dimers closely interacting, but in opposite orientations across the membrane (Fig. 3). The other tetramer (dimer 1 and 2) is related by a two-fold axis perpendicular to the membrane and is formed by the interaction of helices E and D from two adjacent dimers, which create a four-helix bundle (Fig. 3). As these two dimers would have the same orientation in the membrane, it is likely that this tetramer could well exist in vivo in the inner bacterial membrane. At present we must still categorise these oligomers as 'crystallographic tetramers', although once we have assigned amino acid sequences to specific densities, site-directed mutagenesis could be used to assign the interfaces involved in tetramer formation, as has recently been performed for the dimeric transporter, LacS [32]. It also remains to be seen whether there is a functional role for a tetramer in vivo, or whether the dimer is fully capable of catalysing drug efflux.

5. Why is EmrE a dimer and why is it asymmetric?

One rationalisation for why EmrE is a dimer is simply because monomeric EmrE is non-functional, either for substrate binding or for transport. This is suggested from the observation that at low protein concentration the EmrE dimer dissociates with a concomitant loss of functional binding sites [9]. With one TPP$^+$ bound per dimer, it is reasonable to suggest that dimerisation is concurrent with the formation of a functional substrate binding site in EmrE. This is also suggested from biochemical studies on hetero-oligomers [30]. The reason why the EmrE dimer is asymmetric is less certain. One possibility is that the asymmetry may result in slightly different environments for the two essential Glu14 residues in the dimer, which may be important in the transport mechanism. Another possibility is that one or more conformations of a monomer during the transport cycle may be unfavourable, or unstable, but in the dimer that conformation is stabilised and capable of performing its role in the catalytic mechanism. These issues will only be resolved when we have an atomic resolution structure for EmrE and the conformational states of EmrE during the transport cycle have been defined.

6. Note added in proof

A recent publication reported the structure of EmrE at 3.8 Å resolution determined by X-ray diffraction of 3D crystals [Ma, C. and Chang, G. (2004) Proc. Natl. Acad. Sci. USA 101, 2852–2857]. The structure is remarkably different from the structure we have determined by cryo-EM of 2D crystals. Some of the differences may have arisen due to the very different crystallisation conditions needed to produce the 3D crystals, which has resulted in different crystal contacts. In addition, no reference was made in the publication to functional assays on expressed or purified EmrE.

References

[1] Walsh, C. (2000) Nature 406, 775–781.
[2] Nikaido, H. (1994) Science 264, 382–388.
[3] Nikaido, H. (1998) Clin. Infect. Dis. 27 (Suppl. 1), S32–S41.
[4] Paulsen, I.T., Skurray, R.A., Tam, R., Saier Jr., M.H., Turner, R.J., Weiner, J.H., Goldberg, E.B. and Grinius, L.L. (1996) Mol. Microbiol. 19, 1167–1175.
[5] Ninio, S., Rotem, D. and Schuldiner, S. (2001) J. Biol. Chem. 276, 48250–48256.
[6] Schuldiner, S., Granot, D., Mordoch, S.S., Ninio, S., Rotem, D., Soskin, M., Tate, C.G. and Yerushalmi, H. (2001) News Physiol. Sci. 16, 130–134.
[7] Yerushalmi, H., Lebendiker, M. and Schuldiner, S. (1995) J. Biol. Chem. 270, 6856–6863.
[8] Tate, C.G., Kunji, E.R., Lebendiker, M. and Schuldiner, S. (2001) EMBO J. 20, 77–81.
[9] Tate, C.G., Ubarretxena-Belandia, I. and Baldwin, J.M. (2003) J. Mol. Biol. 332, 229–242.
[10] Ubarretxena-Belandia, I., Baldwin, J.M., Schuldiner, S. and Tate, C.G. (2003) EMBO J. 22, 6175–6181.
[11] Morimyo, M., Hongo, E., Hama-Inaba, H. and Machida, I. (1992) Nucleic Acids Res. 20, 3159–3165.
[12] Purewal, A.S. (1991) FEMS Microbiol. Lett. 66, 229–231.
[13] Muth, T.R. and Schuldiner, S. (2000) EMBO J. 19, 234–240.
[14] Mordoch, S.S., Granot, D., Lebendiker, M. and Schuldiner, S. (1999) J. Biol. Chem. 274, 19480–19486.
[15] Yerushalmi, H. and Schuldiner, S. (2000) Biochemistry 39, 14711–14719.
[16] Yerushalmi, H. and Schuldiner, S. (2000) FEBS Lett. 476, 93–97.
[17] Yerushalmi, H., Mordoch, S.S. and Schuldiner, S. (2001) J. Biol. Chem. 276, 12744–12748.
[18] Gutman, N., Steiner-Mordoch, S. and Schuldiner, S. (2003) J. Biol. Chem. 278, 16082–16087.
[19] Koteiche, H.A., Reeves, M.D. and McHaourab, H.S. (2003) Biochemistry 42, 6099–6105.
[20] Soskine, M., Steiner-Mordoch, S. and Schuldiner, S. (2002) Proc. Natl. Acad. Sci. USA 99, 12043–12048.
[21] Arkin, I.T., Russ, W.P., Lebendiker, M. and Schuldiner, S. (1996) Biochemistry 35, 7233–7238.
[22] Schwaiger, M., Lebendiker, M., Yerushalmi, H., Coles, M., Groger, A., Schwarz, C., Schuldiner, S. and Kessler, H. (1998) Eur. J. Biochem. 254, 610–619.
[23] Klammt, C., Lohr, F., Schafer, B., Haase, W., Dotsch, V., Ruterjans, H., Glaubitz, C. and Bernhard, F. (2004) Eur. J. Biochem. 271, 568–580.
[24] von Heijne, G. (1986) EMBO J. 5, 3021–3027.
[25] Veenhoff, L.M., Heuberger, E.H. and Poolman, B. (2002) Trends Biochem. Sci. 27, 242–249.
[26] Zottola, R.J., Cloherty, E.K., Coderre, P.E., Hansen, A., Hebert, D.N. and Carruthers, A. (1995) Biochemistry 34, 9734–9747.
[27] Schroers, A., Burkovski, A., Wohlrab, H. and Kramer, R. (1998) J. Biol. Chem. 273, 14269–14276.
[28] Gerchman, Y., Rimon, A., Venturi, M. and Padan, E. (2001) Biochemistry 40, 3403–3412.
[29] Veenhoff, L.M., Heuberger, E.H. and Poolman, B. (2001) EMBO J. 20, 3056–3062.
[30] Rotem, D., Sal-man, N. and Schuldiner, S. (2001) J. Biol. Chem. 276, 48243–48249.
[31] Yerushalmi, H., Lebendiker, M. and Schuldiner, S. (1996) J. Biol. Chem. 271, 31044–31048.
[32] Geertsma, E.R., Duurkens, R.H. and Poolman, B. (2003) J. Mol. Biol. 332, 1165–1174.